ROBUST CONTROLLERS FOR VARIABLE RELUCTANCE MOTORS

MOHAMED ZRIBI AND MUTHANA T. ALRIFAI

Received 12 June 2004 and in revised form 29 September 2004

This paper investigates the control problem of variable reluctance motors (VRMs). VRMs are highly nonlinear motors; a model that takes magnetic saturation into account is adopted in this work. Two robust control schemes are developed for the speed control of a variable reluctance motor. The first control scheme guarantees the uniform ultimate boundedness of the closed loop system. The second control scheme guarantees the exponential stability of the closed loop system. Simulation results of the proposed controllers are presented to illustrate the theoretical developments. The simulations indicate that the proposed controllers work well, and they are robust to changes in the parameters of the motor and to changes in the load.

1. Introduction

The variable reluctance motor is a synchronous motor which is comprised of iron laminations on the stator and rotor and copper phase windings on the stator. Torque is produced by the attraction of the closet rotor poles to the excited poles. In motoring operations, phase excitation is synchronized to rotor position such that the rotor poles are pulled toward the excited stator poles in the direction of rotation. In generating operations, phase excitation is synchronized to rotor position such that the rotor poles are pulled backward toward the excited stator poles in the direction opposite to the rotation.

Variable reluctance motors are almost maintenance free since they do not have mechanical brushes. Also, VRMs are not expensive because they do not have rotor windings or magnets. Moreover, VRMs can produce high torques at low speeds. These characteristics combined with the advancement in power electronics, and the availability of high-speed processors make variable reluctance motors attractive for many general-purpose industrial applications.

However, the variable reluctance motor is characterized by its inherent nonlinearities. Both spatial and magnetic nonlinearities are found in the VRM. Thus, nonlinear control techniques are needed to compensate for the nonlinearities of the motor.

Many nonlinear control techniques have been developed for the control of VRMs; the reader is referred to [1, 2, 3, 4, 5, 6, 8, 9, 10, 11, 12, 13, 14, 15, 16, 17, 18, 19, 21, 22, 23, 24,

Mathematical Problems in Engineering 2005:2 (2005) 195–214
DOI: 10.1155/MPE.2005.195

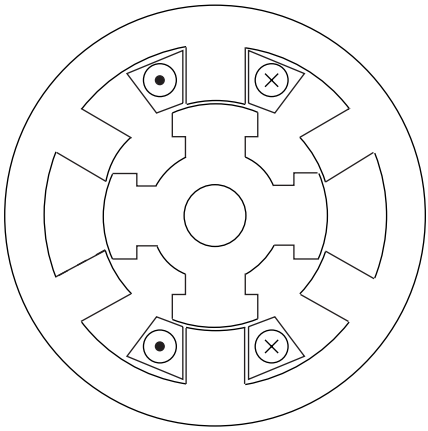

Figure 2.1. A 3-phase, 6/4 VRM. One-phase winding is shown.

25, 26, 27, 28, 29, 30] and the reference therein for an excellent overview of the different control schemes which have been developed for VRMs. Specifically, control techniques such as feedback linearization [13, 22], variable structure control [6], adaptive control [16, 19], optimal control [10], neural control [10], fuzzy control [3, 9, 11], backstepping control [1] have been used for position and speed control of the variable reluctance motor. This paper uses robust nonlinear control techniques to control the speed of the VRM. The need of robust controllers for VRMs is motivated by the inherent nonlinearities of the motor and by the fact that some of the parameters of the motor are not to be known accurately.

The rest of the paper is organized as follows. Section 2 contains a brief overview on variable reluctance motors as well as the dynamic model of the motor. Sections 3 and 4 deal with the design of two controllers for the VRM. The simulation results of the proposed control schemes are presented and discussed in Section 5. Finally the conclusion is given in Section 6.

In the sequel, we denote by W^T the transpose of a matrix or a vector W. We use $W > 0$ ($W < 0$) to denote a positive (negative) definite matrix W. Sometimes, the arguments of a function will be omitted in the analysis when no confusion may arise.

2. Dynamic model of the variable reluctance motor

For any control system design, the development of a reliable mathematical model is essential for proper evaluation of the system's performance and for testing the effectiveness of the developed control schemes. For VRMs, both spatial and magnetic nonlinearities are inherent characteristics of the motor; a model which takes these nonlinearities into account needs to be considered for design purposes. The model suggested in [27] which takes magnetic saturation into account is adopted in this work. A 20 kW, 3-phase VRM, which is documented in [27], is used for simulation purposes. The motor has six stator poles and four rotor poles, see Figure 2.1.

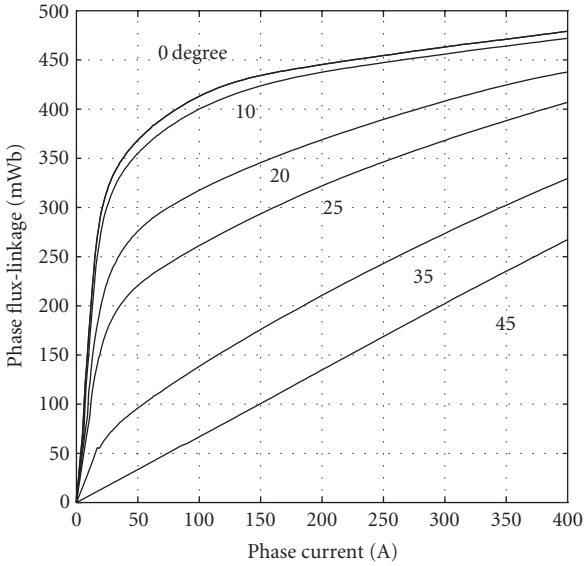

Figure 2.2. The magnetization characteristics of one phase of a 6/4 VRM.

The general voltage equation of an m-phase VRM can be written as

$$v_j = R_j i_j + \frac{d\lambda_j}{dt} \quad (j = 1,2,\ldots,m), \tag{2.1}$$

where v_j $(j = 1,2,\ldots,m)$ is the voltage applied to the terminals of the jth phase, R_j is the phase resistance, i_j $(j = 1,2,\ldots,m)$ is the current associated with phase j, and λ_j $(j = 1,2,\ldots,m)$ is the flux linkage of the jth phase.

The flux linkage λ_j is a nonlinear function of both the phase current i_j and the rotor position θ, see Figure 2.2. The nonlinearities of λ_j are due to the magnetic saturation and to the periodicity of alignment between the stator and the rotor poles. The flux linkage is defined as [27]

$$\lambda(i_j,\theta) = a_{1j}(\theta)\left[1 - \exp\left(a_{2j}(\theta) i_j\right)\right] + a_{3j}(\theta) i_j, \quad i_j \geq 0 \ (j = 1,2,\ldots,m). \tag{2.2}$$

The coefficients a_{1j}, a_{2j}, and a_{3j} $(j = 1,2,\ldots,m)$ are periodic functions of the rotor position, and they can be expressed as truncated Fourier cosine series such that

$$a_k = \sum_{r=0}^{n} A_{kr} \cos(\delta\theta r) \quad (k = 1,2,3), \tag{2.3}$$

where δ is the number of electrical cycles in each mechanical revolution. The parameter A_{kr} represents the rth Fourier coefficient of the kth fitting coefficient. The Fourier coefficients of the VRM are determined by using the Marquardt gradient expansion algorithm [2].

The torque for phase j, T_{ej} $(j = 1,2,\ldots,m)$, produced by a VRM with independent phases during both saturated and unsaturated magnetic operations, can be determined by using coenergy analysis [15] as

$$T_{ej} = \frac{\partial}{\partial\theta}\int_0^{i_j} \lambda(i',\theta)\,di' \quad (j = 1,2,\ldots,m). \tag{2.4}$$

The sum $T_e = \sum_{j=1}^{m} T_{ej}$ of the individual-phase torques gives the total torque.

Therefore, the complete dynamic model of the variable reluctance motor can be written as

$$\begin{aligned} \frac{d\theta}{dt} &= \omega, \\ \frac{d\omega}{dt} &= \frac{1}{J}\{T_e - T_L - D\omega\}, \\ \frac{di_j}{dt} &= \left(\frac{\partial\lambda_j}{\partial i_j}\right)^{-1}\left\{-R_j i_j - \frac{\partial\lambda_j}{\partial\theta}\omega + v_j\right\} \quad (j = 1,2,\ldots,m), \end{aligned} \tag{2.5}$$

where

(i) θ is the rotor position;
(ii) ω is the rotor speed;
(iii) i_j is the current associated with phase j;
(iv) λ_j is the flux linkage of the jth phase;
(v) v_j is the control voltage of the jth phase;
(vi) T_e is the total electromagnetic torque;
(vii) T_L is the load torque;
(viii) J is the rotor inertia;
(ix) D is the damping factor;
(x) R_j is the jth phase resistance.

The output of the system can be taken as the rotor position θ or the rotor speed ω, whereas v_j acts as the control input of the jth phase. This paper deals with speed control, thus the output of the VRM system is $y = \omega$.

Remark 2.1. An electronic commutator determines which phase to be excited at any given instant of time. The inputs to the electronic commutator are the turn-on angle θ_{on}, the turn-off angle θ_{off}, and the rotor position θ; the output of the commutator is the phase to be excited.

For speed control design purposes, the dynamic model of the VRM can be written as

$$\begin{aligned} \frac{d\omega}{dt} &= \frac{1}{J}\{T_e - T_L - D\omega\} = \alpha, \\ \frac{d\alpha}{dt} &= \frac{1}{J}\left\{\sum_{j=1}^{m}\left(\frac{\partial T_{ej}}{\partial i_j}\right)\left(\frac{\partial\lambda_j}{\partial i_j}\right)^{-1}\left(-R_j i_j - \frac{\partial\lambda_j}{\partial\theta}\omega + v_j\right) + \omega\sum_{j=1}^{m}\frac{\partial T_{ej}}{\partial\theta} - T_u - D\alpha\right\}, \end{aligned} \tag{2.6}$$

where $T_u = dT_L/dt$.

Let $x = \binom{x_1}{x_2} = \binom{\omega}{\alpha}$. The model of the VRM system can be written in a compact form as

$$\begin{aligned} \frac{dx_1}{dt} &= x_2, \\ \frac{dx_2}{dt} &= f + gu, \\ y &= x_1, \end{aligned} \tag{2.7}$$

where for a 3-phase VRM, $u = v_j$ ($j = 1$, or 2, or 3) depending on the output of the commutator (i.e., the phase to be excited). The terms f and g are as follows:

$$\begin{aligned} f &= \frac{1}{J}\left\{\sum_{j=1}^{m}\left(\frac{\partial T_{ej}}{\partial i_j}\right)\left(\frac{\partial \lambda_j}{\partial i_j}\right)^{-1}\left(-R_j i_j - \frac{\partial \lambda_j}{\partial \theta}\omega\right) + \omega\sum_{j=1}^{m}\frac{\partial T_{ej}}{\partial \theta} - T_u - D\alpha\right\} \\ &= f_n - \frac{T_u}{J}, \\ g &= \frac{1}{J}\left(\frac{\partial T_{ej}}{\partial i_j}\right)\left(\frac{\partial \lambda_j}{\partial i_j}\right)^{-1}, \quad i = 1,2, \text{ or } 3. \end{aligned} \tag{2.8}$$

Assumption 2.2. The model of the VRM is known as it has been experimentally verified [26, 28]. Therefore the terms f_n and g in the above equations are known. The term T_u in f comprises the rate of change of the torque of the incoming phases and the load torque; this term is considered as an uncertain quantity. Thus, the nonlinear term f is not known exactly but can be written as $f = f_n + \Delta f$, where f_n is the known nominal part of f and Δf is the uncertain part of f. It is assumed that Δf is bounded by a known positive function ρ such that

$$|\Delta f| \leq \rho. \tag{2.9}$$

Remark 2.3. The equation $d\theta/dt = \omega$ is not included in model (2.7) of the VRM system because the paper deals with speed control. Obviously, for a given $\omega(t)$, one can easily find $\theta(t)$ such that $\theta(t) = \theta(0) + \int_0^t \omega(\tau)d\tau$.

Note that at equilibrium, $x_{1e} = \omega_{\text{ref}}$, and $x_{2e} = \alpha_{\text{ref}} = 0$, where ω_{ref} is a constant reference speed command. Define the error $e = \binom{e_1}{e_2}$ where e_1 and e_2 are such that

$$\begin{aligned} e_1 &= x_1 - \omega_{\text{ref}}, \\ e_2 &= x_2 - \alpha_{\text{ref}} = x_2. \end{aligned} \tag{2.10}$$

Using (2.7) and (2.10), the model of the VRM system can be written as

$$\dot{e}_1 = e_2, \tag{2.11}$$

$$\dot{e}_2 = f + gu, \tag{2.12}$$

$$y = x_1. \tag{2.13}$$

The system (2.12) and (2.13) will be used for the design of the control schemes.

3. Design of the first robust control scheme for the VRM

In this section, we propose to use a Corless-/Leitmann-type controller [7] to control the variable reluctance motor.

Define the matrix A and the vector B such that

$$A = \begin{bmatrix} 0 & 1 \\ -k_1 & -k_2 \end{bmatrix}, \qquad B = \begin{bmatrix} 0 \\ 1 \end{bmatrix}, \tag{3.1}$$

where the positive scalars k_1 and k_2 are chosen such that the polynomial $s^2 + k_2 s + k_1$ is Hurwitz.

Let P_1 and Q_1 be symmetric positive definite matrices such that

$$A^T P_1 + P_1 A = -Q_1 \tag{3.2}$$

and let ϵ be a small positive scalar. In addition, define μ_1 such that

$$\mu_1 = \rho B^T P_1 e. \tag{3.3}$$

Definition 3.1 [12]. The error e is said to be uniformly ultimately bounded if there exist constants b and c, and for every $r \in (0,c)$ there is a constant $T = T(r) \geq 0$ such that

$$||e(t_0)|| < r \Longrightarrow ||e(t)|| < b, \quad \forall t > t_0 + T. \tag{3.4}$$

The following proposition gives the main result of this section.

Proposition 3.2. *The control law*

$$u = -\frac{1}{g}(f_n + k_1 e_1 + k_2 e_2) + \frac{1}{g} u_{c_1} \tag{3.5}$$

with

$$u_{c_1} = \begin{cases} -\dfrac{\mu_1}{||\mu_1||}\rho & \text{if } ||\mu_1|| > \epsilon, \\ -\dfrac{\mu_1}{\epsilon}\rho & \text{if } ||\mu_1|| \leq \epsilon \end{cases} \tag{3.6}$$

when applied to the VRM system (2.12) and (2.13) guarantees the uniform ultimate boundedness of the closed loop system.

Proof. Using (2.12), (3.1), and (3.4), the closed loop system can be written as

$$\dot{e} = Ae + Bu_{c_1} + B\Delta f. \tag{3.7}$$

Consider the following Lyapunov function candidate V_1:

$$V_1 = e^T P_1 e. \tag{3.8}$$

Note that $V_1 > 0$ for $e \neq 0$ and $V_1 = 0$ for $e = 0$.

Equation (3.7) implies that $\lambda_1 \|e\|^2 \leq V_1 \leq \lambda_2 \|e\|^2$, where λ_1 is the minimum eigenvalue of P_1 and λ_2 is the maximum eigenvalue of P_1.

Taking the derivative of V_1 with respect to time and using (3.6) and (3.2), it follows that

$$\begin{aligned}
\dot{V}_1 &= \dot{e}^T P_1 e + e^T P_1 \dot{e} \\
&= \left(Ae + Bu_{c_1} + B\Delta f\right)^T P_1 e + e^T P_1 \left(Ae + Bu_{c_1} + B\Delta f\right) \\
&= e^T \left(A^T P_1 + P_1 A\right) e + 2e^T P_1 B u_{c_1} + 2\Delta f B^T P_1 e \\
&= -e^T Q_1 e + 2e^T P_1 B u_{c_1} + 2\Delta f B^T P_1 e.
\end{aligned} \tag{3.9}$$

For the case when $\|\mu_1\| > \epsilon$, we have $u_{c_1} = (-\mu_1/\|\mu_1\|)\rho$. Hence, the above equation leads to

$$\begin{aligned}
\dot{V}_1 &= -e^T Q_1 e - 2\frac{e^T P_1 B \mu_1}{||\mu_1||}\rho + 2\Delta f B^T P_1 e \\
&= -e^T Q_1 e - 2\frac{||B^T P_1 e||^2}{||B^T P_1 e||}\rho + 2\Delta f B^T P_1 e \\
&\leq -e^T Q_1 e - 2||B^T P_1 e||\rho + 2|\Delta f|\,||B^T P_1 e|| \\
&\leq -e^T Q_1 e \\
&\leq -\lambda_3 \|e\|^2,
\end{aligned} \tag{3.10}$$

where λ_3 is the minimum eigenvalue of Q_1.

For the case when $\|\mu_1\| \leq \epsilon$, we have $u_{c_1} = (-\mu_1/\epsilon)\rho$. Hence, (3.8) leads to

$$\begin{aligned}
\dot{V}_1 &= -e^T Q_1 e - 2\frac{e^T P_1 B \mu_1}{\epsilon}\rho + 2\Delta f B^T P_1 e \\
&= -e^T Q_1 e - 2\frac{||B^T P_1 e||^2}{\epsilon}\rho^2 + 2\Delta f B^T P_1 e \\
&\leq -e^T Q_1 e - 2\frac{||B^T P_1 e||^2}{\epsilon}\rho^2 + 2|\Delta f|\,||B^T P_1 e|| \\
&\leq -e^T Q_1 e + 2||B^T P_1 e||\rho \\
&\leq -e^T Q_1 e + 2\epsilon \\
&\leq -\lambda_3 \|e\|^2 + 2\epsilon.
\end{aligned} \tag{3.11}$$

Therefore, it can be concluded that for all t and all x, we have

$$\dot{V}_1 \leq -\lambda_3 \|e\|^2 + 2\epsilon. \tag{3.12}$$

Let $\kappa = \lambda_3/\lambda_2$, it follows that

$$\dot{V}_1 \leq -\kappa V_1 + 2\epsilon. \tag{3.13}$$

Therefore, it can be concluded that V_1 decreases monotonically along any trajectory of the closed loop system until it reaches the compact set

$$\Lambda_s = \left\{ e \mid V_1 \leq V_s = \frac{2\epsilon}{\kappa} \right\}. \tag{3.14}$$

Hence the trajectories of the closed loop system of the VRM are uniformly ultimately bounded with respect to the bound ϵ. □

4. Design of the second robust control scheme for the VRM

The controller proposed in the previous section can only guarantee the uniform ultimate boundedness of the closed loop system. In this section, a second nonlinear state feedback controller is proposed. This controller is similar to the Corless-/Leitmann-type controller in that it works well for a class of nonlinear uncertain systems that have matched uncertainties which are bounded by some known continuous-time functions. However, this control scheme, which is motivated by the work in [20], has the advantage of guaranteeing the exponential stability of the closed loop system.

Let P_2 and Q_2 be symmetric positive definite matrices which are solutions to the algebraic Riccati equation

$$A^T P_2 + P_2 A - 2P_2 B B^T P_2 = -Q_2 \tag{4.1}$$

and let

$$\mu_2 = \rho B^T P_2 e \tag{4.2}$$

and

$$\vartheta = \frac{\mu_2 ||\mu_2||^2}{||\mu_2||^3 + \varepsilon^3 \exp(-3\beta t)} \rho \tag{4.3}$$

with ε and β being positive scalars.

Definition 4.1 [12]. The error e is said to be exponentially stable if

$$||e(t_0)|| < c \Longrightarrow ||e(t)|| \leq \overline{\beta} ||e(t_0)|| \exp(\overline{\gamma}(t - t_0)), \quad \forall t \geq t_0 \geq 0, \text{ with } \overline{\beta} > 0,\ \overline{\gamma} > 0. \tag{4.4}$$

The following proposition gives the result of this section.

Proposition 4.2. *The control law*

$$u = -\frac{1}{g}(f_n + k_1 e_1 + k_2 e_2) + \frac{1}{g}u_{c_2} \tag{4.5}$$

with

$$u_{c_2} = -B^T P_2 e - \vartheta \tag{4.6}$$

when applied to the VRM system guarantees the exponential stability of the closed loop system.

Proof. The closed loop system can be written as

$$\dot{e} = Ae + Bu_{c_2} + B\Delta f. \tag{4.7}$$

Using (4.4) and (4.5), it follows that

$$\begin{aligned} \dot{e}^T P_2 e &= \left(Ae + B\left(-B^T P_2 e - \vartheta\right) + B\Delta f\right)^T P_2 e \\ &= \left(e^T A^T - e^T P_2 B B^T - B^T \vartheta + B^T \Delta f\right) P_2 e. \end{aligned} \tag{4.8}$$

Consider the following Lyapunov function candidate V_2:

$$V_2 = e^T P_2 e. \tag{4.9}$$

Note that $V_2 > 0$ for $e \neq 0$ and $V_2 = 0$ for $e = 0$.

Equation (4.7) implies that $\lambda_1' \|e\|^2 \leq V_2 \leq \lambda_2' \|e\|^2$, where λ_1' is the minimum eigenvalue of P_2 and λ_2' is the maximum eigenvalue of P_2.

Taking the derivative of V_2 with respect to time and using (4.6), (3.14), and (4.2), it follows that

$$\begin{aligned} \dot{V}_2 &= \dot{e}^T P_2 e + e^T P_2 \dot{e} \\ &= e^T \left(A^T P_2 + P_2 A - 2P_2 B B^T P_2\right) e - 2e^T P_2 B\vartheta + 2e^T P_2 B\Delta f \\ &= -e^T Q_2 e - 2e^T P_2 B\vartheta + 2e^T P_2 B\Delta f \\ &= -e^T Q_2 e - \frac{2e^T P_2 B\mu_2 ||\mu_2||^2}{||\mu_2||^3 + \varepsilon^3 \exp(-3\beta t)}\rho + 2e^T P_2 B\Delta f \\ &\leq -e^T Q_2 e - \frac{2||B^T P_2 e||^4 \rho^4}{||B^T P_2 e||^3 \rho^3 + \varepsilon^3 \exp(-3\beta t)} + 2||B^T P_2 e||\rho \\ &\leq -e^T Q_2 e + \frac{2||B^T P_2 e||\rho\varepsilon^3 \exp(-3\beta t)}{||B^T P_2 e||^3 \rho^3 + \varepsilon^3 \exp(-3\beta t)} \\ &\leq -e^T Q_2 e + 2\varepsilon \exp(-\beta t) \\ &\leq -\lambda_3' \|e\|^2 + 2\varepsilon \exp(-\beta t), \end{aligned} \tag{4.10}$$

Table 5.1. Parameters of the VRM.

Parameter	Value
Output power	20 kW
Rated speed	492 rad/s
Number of phases (m)	3
Number of stator poles	6
Number of rotor poles	4
Aligned phase inductance (L_a)	19.0 mH
Unaligned phase inductance (L_u)	0.67 mH
Rotor inertia (J)	0.02 Nm s^2
Damping factor (D)	0.3301×10^{-3} Nm s
Phase resistance (R)	0.069 Ω
DC voltage supply	230 V

where the fact that $0 \le ab^3/(a^3+b^3) \le b$ for $a, b \ge 0$ and $a^3+b^3 \ne 0$ was used; and λ_3' is the minimum eigenvalue of Q_2.

Let $\kappa' = \lambda_3'/\lambda_2'$, it follows that

$$\dot{V}_2 \le -\kappa' V_2 + 2\varepsilon \exp(-\beta t). \tag{4.11}$$

Thus, it can be concluded that the error $e(t)$ is globally exponentially stable. Moreover, the convergence rate of the errors is such that

$$||e(t)|| \le \begin{cases} \left[\dfrac{\lambda_2'}{\lambda_1'}||e(0)||^2 \exp(-\kappa' t) + \dfrac{2\varepsilon}{\lambda_1'} t \exp(-\kappa' t)\right]^{1/2} & \text{if } \beta = \kappa', \\ \left[\dfrac{\lambda_2'}{\lambda_1'}||e(0)||^2 \exp(-\kappa' t) + \dfrac{2\varepsilon}{\lambda_1'(\kappa'-\beta)}\left(\exp(-\beta t) - \exp(-\kappa' t)\right)\right]^{1/2} & \text{if } \beta \ne \kappa'. \end{cases} \tag{4.12}$$

□

5. Simulation results of the proposed controllers

The VRM system is simulated using the Matlab software. The VRM model discussed in Section 2 is adopted; the model takes magnetic saturation into account.

The parameters of the motor are given in Table 5.1.

The excitation angles (θ_{on} and θ_{off}) are kept fixed throughout the simulation studies at 45° and 79°, respectively, (where 0° and 90° correspond to aligned and unaligned positions). Only one phase is allowed to be excited at one time.

Simulations are performed when the proposed controllers are applied to the VRM system. The results are presented in the following subsections.

5.1. Performance of the VRM system when the first controller is used. The control scheme given by (3.4) and (3.5) is applied to the VRM system. The desired speed is 100 rad/s for $0 \le t < 0.1$ seconds, and it is 200 rad/s for $0.1 \le t \le 0.2$ seconds. The load

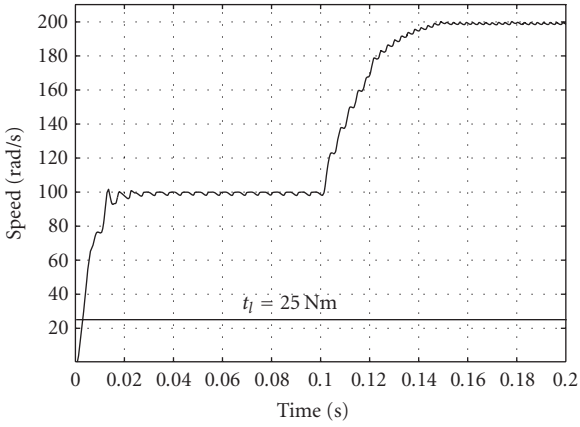

Figure 5.1. Speed response of the VRM when the first controller is used.

torque is taken to be 25 Nm. Figure 5.1 shows the speed response of the motor. It can be seen from the figure that the motor speed converges to the desired speeds. It should be mentioned that the ripples in the speed response are due to the sequential switching between the phases and they are not caused by the controller.

5.2. Performance of the VRM system when the second controller is used. The control law described by (4.3) and (4.4) is applied to the VRM system. Figure 5.7 shows the speed response of the motor when it is commanded to accelerate from rest to a reference speed of 100 rad/s then to 200 rad/s, with a load torque of 25 Nm. It can be seen that the motor speed converges to the desired speeds. The ripples in the speed response are due to the motor operational characteristics and limits of the electronic commutator; the ripples are not due to the proposed controller.

Remark 5.1. The VRM used for simulation studies is a 3-phase 6/4 motor. The low number of poles will have a negative impact on the produced torque of the motor. As a result, the speed will be affected and hence the response of the speed will have more ripples.

5.3. Robustness of the proposed control schemes. Simulation studies are undertaken to test the robustness of the proposed controllers to variations in the parameters. Changes in the phase resistance R, the rotor inertia J, the damping factor D, and the a_{1j}, a_{2j}, and a_{3j} $(j = 1,2,\ldots,m)$ coefficients (which are used to model the phase flux-linkage) are investigated. The simulations are carried out by step changing one parameter at a time while keeping the other parameters unchanged. The step change occurs at time $t = 0.1$ seconds and at time $t = 0.15$ seconds. The motor is commanded to accelerate from rest to a reference speed of 200 rad/s with a load torque of 25 Nm.

Figures 5.2–5.5 and 5.8–5.11 show the motor responses when there are changes in the parameters of the VRM system. Figure 5.2 (first controller) and Figure 5.8 (second controller) show the responses of the motor when the phase resistance is increased to 200%

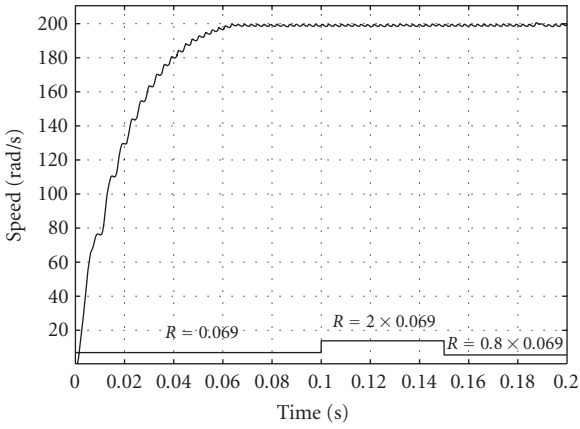

Figure 5.2. Speed response of the VRM when the first controller is used with changes in R.

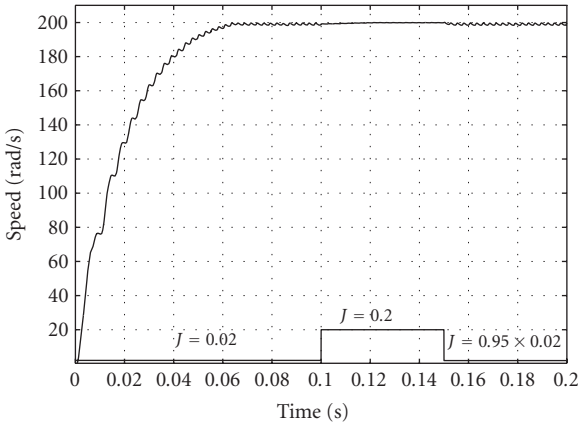

Figure 5.3. Speed response of the VRM when the first controller is used with changes in J.

of its original value and then decreased to 80% of its original value. Figure 5.3 (first controller) and Figure 5.9 (second controller) show the responses of the motor when the rotor inertia is varied by up to 10 times its original value. Figure 5.4 (first controller) and Figure 5.10 (second controller) show the responses of the motor when the damping factor is varied by up to 10 times its original value. Figure 5.5 (first controller) and Figure 5.11 (second controller) show the responses of the motor when the a_{1j}, a_{2j}, and a_{3j} $(j = 1,2,\ldots,m)$ coefficients are increased to 110% of their original values and then decreased to 90% of their original values; the change in the coefficients is only 10% because these coefficients are usually known quite accurately from experimental studies. Hence, it can be concluded from the simulation results that the proposed controllers are robust to changes in the parameters of the system.

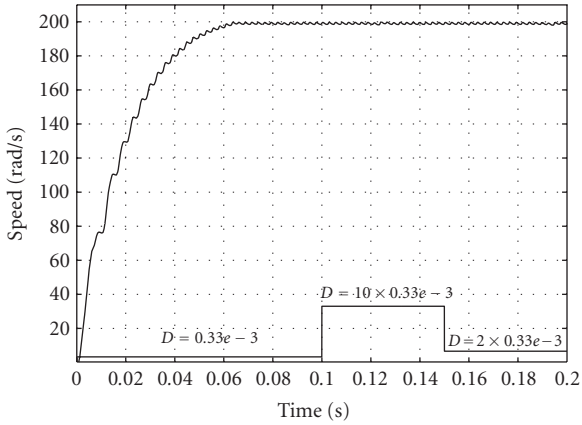

Figure 5.4. Speed response of the VRM when the first controller is used with changes in D.

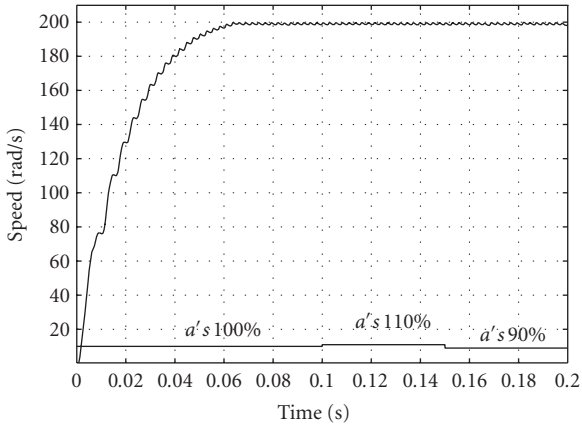

Figure 5.5. Speed response of the VRM when the first controller is used with changes in the $a'_{ij}s$ coefficients.

It is desirable for high-performance applications that the proposed control schemes be robust to variations in the load torque. Simulation studies are carried out to demonstrate the robustness of the proposed controllers to changes in the load torque. The motor is commanded to accelerate from rest to 200 rad/s. Figure 5.6 (first controller) and Figure 5.12 (second controller) show the motor responses when the load torque changes from 25 Nm to 50 Nm and back to 25 Nm. It can be seen from these two figures that the motor responses have a dip in speed when the load is suddenly changed, but both controllers are able to keep the motor speed close to the desired speed. Therefore, it can be concluded that the proposed controllers are robust to changes in the load.

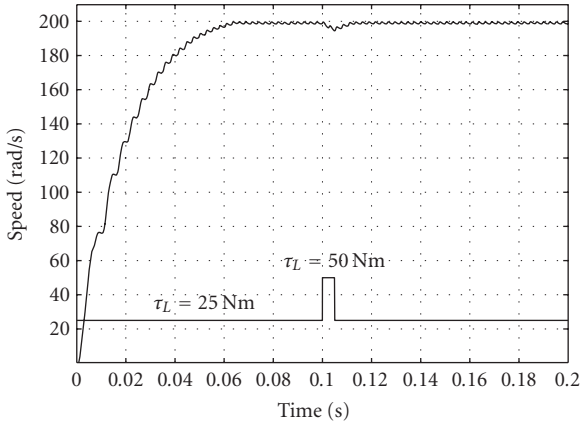

Figure 5.6. Speed response of the VRM when the first controller is used with changes in the load torque.

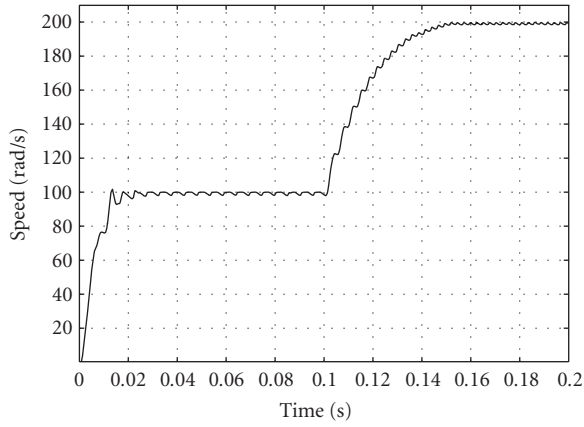

Figure 5.7. Speed response of the VRM when the second controller is used.

5.4. Comparison of the proposed control schemes with a PI controller and a feedback linearization controller. The performance of the closed loop system is compared to the performance of the system when (1) a proportional plus integral (PI) controller is used, and (2) a feedback linearization controller is used. The choice of the PI controller is motivated by the fact that the PI controller is usually used in industrial VRMs. The choice of the feedback linearization controller is due to the simplicity of the design of this type of controllers.

The equation of the PI controller is as follows:

$$u = K_p(\omega - \omega_{\text{ref}}) + K_I \int (\omega - \omega_{\text{ref}})\, dt = K_p e_1 + K_I \int e_1\, dt. \tag{5.1}$$

The gains K_p and K_I are tuned using the trial and error method.

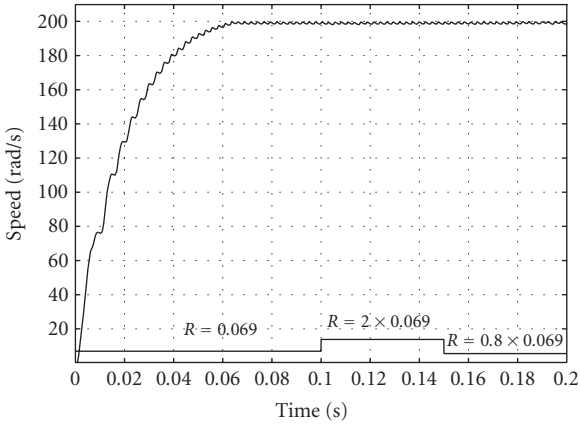

Figure 5.8. Speed response of the VRM when the second controller is used with changes in R.

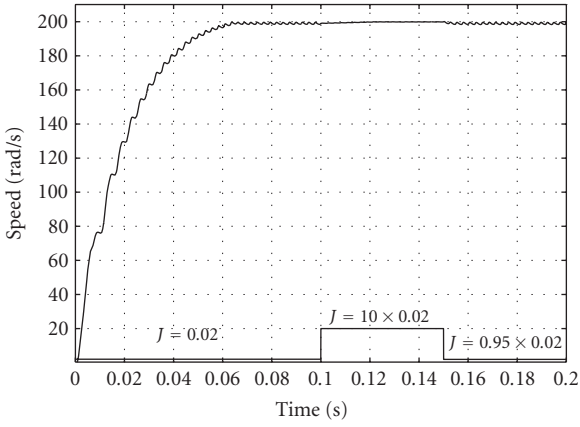

Figure 5.9. Speed response of the VRM when the second controller is used with changes in J.

The control scheme given by (5.1) is applied to the VRM system. The desired speed is 100 rad/s for $0 \le t < 0.1$ seconds, and it is 200 rad/s for $0.1 \le t \le 0.2$ seconds; the load torque is taken to be 25 Nm. Figure 5.13 shows the speed response of the motor. It can be seen from the figure that the motor speed converges to the desired speeds.

Recall that the model of the VRM system can be written as

$$\begin{aligned} \dot{e}_1 &= e_2, \\ \dot{e}_2 &= f + gu, \\ y &= x_1. \end{aligned} \tag{5.2}$$

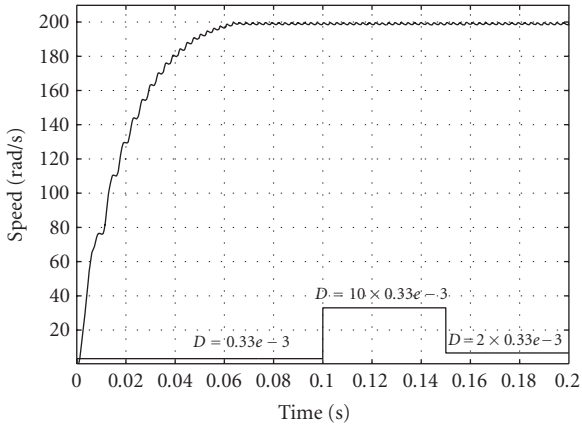

Figure 5.10. Speed response of the VRM when the second controller is used with changes in D.

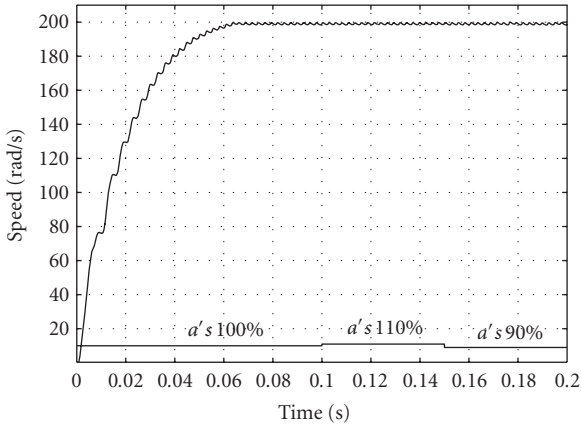

Figure 5.11. Speed response of the VRM when the second controller is used with changes in the $a'_{ij}s$ coefficients.

A feedback linearization controller for the above system can be written as

$$u = -\frac{1}{g}(f + k_1 e_1 + k_2 e_2), \tag{5.3}$$

where k_1 and k_2 are properly designed gains. The value of f is taken to be the nominal value.

The control scheme given by (5.3) is applied to the VRM system. Figure 5.14 shows the speed response of the motor. It can be seen from the figure that the motor speed converges to the desired speeds.

Figures 5.13 and 5.14 show the responses of the VRM system when the PI controller, the feedback linearization controller, and the two proposed controllers are used. It can

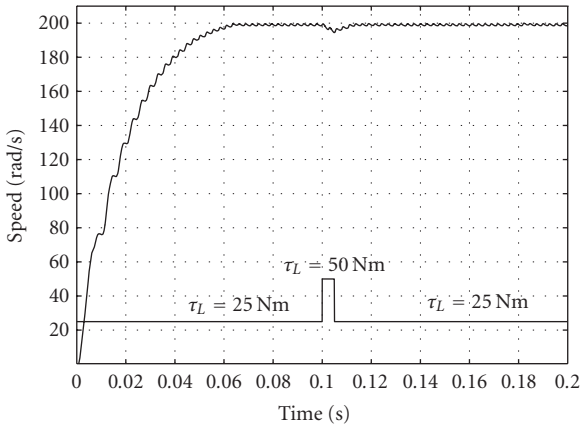

Figure 5.12. Speed response of the VRM when the second controller is used with changes in the load torque.

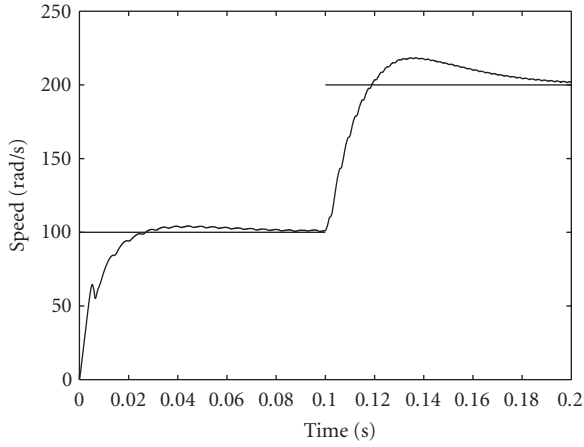

Figure 5.13. Speed response of the VRM when the PI controller is used.

be seen that the four controllers force the speed of the motor to converge to the desired speeds. However, it can be seen from the figures that the proposed controllers gave better results than the PI controller or the feedback linearization controller. This is an expected result as the PI controller is a simple controller to design and to implement. The design of the feedback linearization controller did not take the uncertainties of the VRM system into account and hence it did not perform as well as the two proposed controllers. In addition, the second controller gave slightly better results than the first controller (as can be seen from Figure 5.14) since the first controller guarantees the uniform ultimate boundedness of the system and the second controller guarantees the exponential stability of the system.

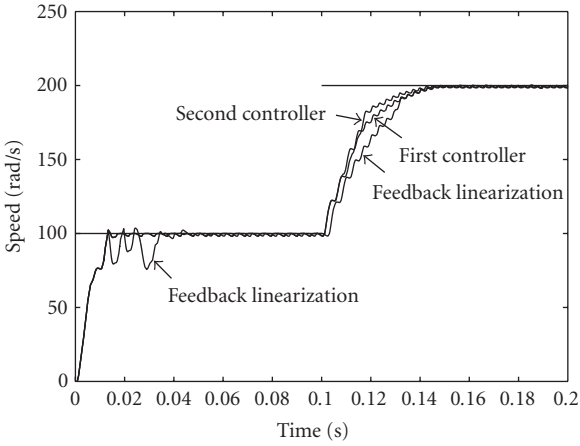

Figure 5.14. Speed response of the VRM when the feedback linearization controller, the first controller, and the second controller are used.

6. Conclusion

In this paper, two control schemes are designed for the speed control of variable reluctance motors. The first proposed controller guarantees the uniform ultimate boundedness of the closed loop system; the second controller guarantees the exponential stability of the closed loop system. A highly nonlinear model is adopted for the design of the controllers, this model takes magnetic saturation into account. The proposed controllers are based on varying the terminal voltage of the motor using a DC-DC chopper. The inputs to the controllers are the phase currents, the rotor position, and the speed of the motor. The performances of the controllers are illustrated through simulations. The results indicate that the proposed control schemes are able to bring the motor speed to the desired speed. Moreover, the simulation results show the robustness of the proposed controllers to changes in the parameters of a motor and to changes in the load. Future work will address the implementation of the proposed control schemes using a DSP-based digital controller board.

Acknowledgment

This research was supported by Kuwait University under research Grant no. EE 03/02.

References

[1] M. T. Alrifai, J. H. Chow, and D. A. Torrey, *Backstepping nonlinear speed controller for switched-reluctance motors*, Elec. Power App. **150** (2003), no. 2, 193–200.

[2] P. R. Bevington, *Data Reduction and Error Analysis for the Physical Sciences*, McGraw-Hill, New York, 1969.

[3] S. Bolognani and M. Zigliotto, *Fuzzy logic control of a switched reluctance motor drive*, IEEE Trans. Ind. Applicat. **32** (1996), no. 5, 1063–1068.

[4] S. A. Bortoff, R. R. Kohan, and R. Milman, *Adaptive control of variable reluctance motors: a spline function approach*, IEEE Trans. Ind. Electron. **45** (1998), no. 3, 433–444.

[5] E. Capecchi, P. Gugliehni, M. Pastorelli, and A. Vagati, *Position-sensorless control of the transverse-laminated synchronous reluctance motor*, IEEE Trans. Ind. Applicat. **37** (2001), no. 6, 1768–1776.

[6] T.-S. Chuang and C. Pollock, *Robust speed control of a switched reluctance vector drive using variable structure approach*, IEEE Trans. Ind. Electron. **44** (1997), no. 6, 800–808.

[7] M. J. Corless and G. Leitmann, *Continuous state feedback guaranteeing uniform ultimate boundedness for uncertain dynamic systems*, IEEE Trans. Automat. Contr. **26** (1981), no. 5, 1139–1144.

[8] W. D. Harris and J. H. Lang, *A simple motion estimator for variable-reluctance motors*, IEEE Trans. Ind. Applicat. **26** (1990), no. 2, 237–243.

[9] K. I. Hwu and C. M. Liaw, *Quantitative speed control for SRM drive using fuzzy adapted inverse model*, IEEE Trans. Aerosp. Electron. Syst. **38** (2002), no. 3, 955–968.

[10] F. Ismail, S. Wahsh, A. Mohamed, and H. Elsimary, *Optimal control of variable reluctance motor by neural network*, Proceedings of the IEEE International Symposium on Industrial Electronics (ISIE '93) (Budapest), 1993, pp. 301–304.

[11] F. Ismail, S. Wahsh, and A. Z. Mohamed, *Fuzzy-neuro based optimal control of variable reluctance motor*, Proc. 4th IEEE Conference on Control Applications (New York), 1995, pp. 768–773.

[12] H. K. Khalil, *Nonlinear Systems*, Macmillan Publishing, New York, 1992.

[13] C.-H. Kim and I.-J. Ha, *A new approach to feedback-linearizing control of variable reluctance motors for direct-drive applications*, IEEE Trans. Contr. Syst. Technol. **4** (1996), no. 4, 348–362.

[14] C. G. Lo Bianco, A. Tonielli, and F. Filicori, *A prototype controller for variable reluctance motors*, IEEE Trans. Ind. Electron. **43** (1996), no. 1, 207–216.

[15] P. Materu and R. Krishnan, *Estimation of switched reluctance motor losses*, Proc. IEEE Conference Record of the Industry Applications Society Annual Meeting (Pennsylvania), vol. 1, 1988, pp. 79–90.

[16] H. Melkote, F. Khorrami, S. Jain, and M. S. Mattice, *Robust adaptive control of variable reluctance stepper motors*, IEEE Trans. Contr. Syst. Technol. **7** (1999), no. 2, 212–221.

[17] A. M. Michaelides and C. Pollock, *Modelling and design of switched reluctance motors with two phases simultaneously excited*, Elec. Power App. **143** (1996), no. 5, 361–370.

[18] T. J. E. Miller, *Brushless Permanent-Magnet and Reluctance Motor Drives*, Clarendon Press, Oxford, 1989.

[19] R. Milman and S. A. Bortoff, *Observer-based adaptive control of a variable reluctance motor: experimental results*, IEEE Trans. Contr. Syst. Technol. **7** (1999), no. 5, 613–621.

[20] S. K. Nguang and M. Fu, *Global quadratic stabilization of a class of nonlinear systems*, Internat. J. Robust Nonlinear Control **8** (1998), no. 6, 483–497.

[21] S. K. Panda, K. Y. Chong, and K. S. Lock, *Indirect rotor position sensing for variable reluctance motors*, Proc. IEEE Conference Record of the Industry Applications Society Annual Meeting (Colorado), vol. 1, 1994, pp. 644–648.

[22] S. K. Panda and P. K. Dash, *Application of nonlinear control to switched reluctance motors: a feedback linearisation approach*, Elec. Power App. **143** (1996), no. 5, 371–379.

[23] C. Pollock and A. M. Michaelides, *Switched reluctance drives: a comparative evaluation*, Power Engineering Journal **9** (1995), no. 6, 257–266.

[24] M. M. Rayan, M. M. Mansour, M. A. El-Sayad, and M. S. Morsy, *Implementation and testing of a digital controller for variable reluctance motor*, Proc. IEEE 14th Annual Applied Power Electronics Conference and Exposition (APEC '99) (Texas), vol. 1, 1999, pp. 430–433.

[25] C. Rossi, A. Tonielli, C. G. Lo Bianco, and F. Filicori, *Robust control of a variable reluctance motor*, Proc. IEEE/RSJ International Workshop on Intelligent Robots and Systems. Intelligence for Mechanical Systems (IROS '91) (Osaka), vol. 1, 1991, pp. 337–343.

[26] D. A. Torrey, *An experimentally verified variable-reluctance machine model implemented in the Saber circuit simulator*, Electric Machines and Power Systems **24** (1996), 199–210.
[27] D. A. Torrey and J. H. Lang, *Modelling a nonlinear variable-reluctance motor drive*, Elec. Power App. **137** (1990), no. 5, 314–326.
[28] D. A. Torrey, X.-M. Niu, and E. J. Unkauf, *Analytical modelling of variable-reluctance machine magnetisation characteristics*, Elec. Power App. **142** (1995), no. 1, 14–22.
[29] I.-W. Yang and Y.-S. Kim, *Rotor speed and position sensorless control of a switched reluctance motor using the binary observer*, Elec. Power App. **147** (2000), no. 3, 220–226.
[30] L.-C. R. Zai, D. G. Manzer, and C.-Y. D. Wong, *High-speed control of variable reluctance motors with reduced torque ripple*, Proc. 7th Annual Applied Power Electronics Conference and Exposition (APEC '92) (Massachusetts), 1992, pp. 107–113.

Mohamed Zribi: Department of Electrical Engineering, College of Engineering & Petroleum, Kuwait University, P. O. Box 5969, Safat 13060, Kuwait
E-mail address: mzribi@eng.kuniv.edu.kw

Muthana T. Alrifai: Department of Electrical Engineering, College of Engineering & Petroleum, Kuwait University, P. O. Box 5969, Safat 13060, Kuwait
E-mail address: alrifm@eng.kuniv.edu.kw

Journal of Applied Mathematics and Decision Sciences

Special Issue on Decision Support for Intermodal Transport

Call for Papers

Intermodal transport refers to the movement of goods in a single loading unit which uses successive various modes of transport (road, rail, water) without handling the goods during mode transfers. Intermodal transport has become an important policy issue, mainly because it is considered to be one of the means to lower the congestion caused by single-mode road transport and to be more environmentally friendly than the single-mode road transport. Both considerations have been followed by an increase in attention toward intermodal freight transportation research.

Various intermodal freight transport decision problems are in demand of mathematical models of supporting them. As the intermodal transport system is more complex than a single-mode system, this fact offers interesting and challenging opportunities to modelers in applied mathematics. This special issue aims to fill in some gaps in the research agenda of decision-making in intermodal transport.

The mathematical models may be of the optimization type or of the evaluation type to gain an insight in intermodal operations. The mathematical models aim to support decisions on the strategic, tactical, and operational levels. The decision-makers belong to the various players in the intermodal transport world, namely, drayage operators, terminal operators, network operators, or intermodal operators.

Topics of relevance to this type of decision-making both in time horizon as in terms of operators are:

- Intermodal terminal design
- Infrastructure network configuration
- Location of terminals
- Cooperation between drayage companies
- Allocation of shippers/receivers to a terminal
- Pricing strategies
- Capacity levels of equipment and labour
- Operational routines and lay-out structure
- Redistribution of load units, railcars, barges, and so forth
- Scheduling of trips or jobs
- Allocation of capacity to jobs
- Loading orders
- Selection of routing and service

Before submission authors should carefully read over the journal's Author Guidelines, which are located at http://www.hindawi.com/journals/jamds/guidelines.html. Prospective authors should submit an electronic copy of their complete manuscript through the journal Manuscript Tracking System at http://mts.hindawi.com/, according to the following timetable:

Manuscript Due	June 1, 2009
First Round of Reviews	September 1, 2009
Publication Date	December 1, 2009

Lead Guest Editor

Gerrit K. Janssens, Transportation Research Institute (IMOB), Hasselt University, Agoralaan, Building D, 3590 Diepenbeek (Hasselt), Belgium; Gerrit.Janssens@uhasselt.be

Guest Editor

Cathy Macharis, Department of Mathematics, Operational Research, Statistics and Information for Systems (MOSI), Transport and Logistics Research Group, Management School, Vrije Universiteit Brussel, Pleinlaan 2, 1050 Brussel, Belgium; Cathy.Macharis@vub.ac.be